Universal Algebraic Relaxation of Velocity and Phase in Pulled
Fronts Generating Periodic or Chaotic States

C. Storm, W. Spruijt, U. Ebert, W. van Saarloos

Universal Algebraic Relaxation of Velocity and Phase
in Pulled Fronts Generating Periodic or Chaotic States

Cornelis Storm[1], Willem Spruijt[1], Ute Ebert[1,2] and Wim van Saarloos[1]

[1]*Instituut–Lorentz, Universiteit Leiden, Postbus 9506, 2300 RA Leiden, The Netherlands*
[2]*CWI, Postbus 94079, 1090 GB Amsterdam, The Netherlands*

ABSTRACT

We investigate the asymptotic relaxation of so-called pulled fronts propagating into an unstable state. The "leading edge representation" of the equation of motion reveals the universal nature of their propagation mechanism and allows us to generalize the universal algebraic velocity relaxation of uniformly translating fronts to fronts, that generate periodic or even chaotic states. Such fronts in addition exhibit a universal algebraic phase relaxation. We numerically verify our analytical predictions for the Swift-Hohenberg and the Complex Ginzburg-Landau equation.

1

Many systems, when driven sufficiently far from equilibrium, spontaneously organize themselves in coherent or incoherent patterns. The ubiquity of such structures in almost all fields of the natural sciences [1,2] has inspired much of the recent scientific effort to uncover the various mechanisms underlying their behavior. Especially in physics, the insight from the seventies that in critical phenomena universality classes are determined essentially by the symmetry of the order parameter and the dimensionality, initially raised some hopes that there would be analogous broad universality classes in nonequilibrium pattern formation. Over the last two decades, it has become clear, however, that such far-reaching universality does not exist: While there *are* various general dynamical and instability mechanisms, there is not always a sharp selection mechanism. Moreover, if there is sharp selection, the particular mechanism may depend on the specific boundary conditions, initial conditions, etc.

In the case of front propagation, there have, nevertheless, been several hints of a generic dynamical mechanism [3,4]: There is a large class of fronts propagating into an unstable state whose asymptotic velocity equals v^*, the asymptotic spreading velocity of linear perturbations about the unstable state. Such fronts are called *pulled* fronts, as they are "pulled along" by the leading edge of the profile whose dynamics is governed by the linearization about the unstable state [5–7]. It is the purpose of this letter to show that within the subclass of pulled front propagation, a remarkable degree of universality does hold: Irrespective of whether such fronts are uniformly translating or generate periodic or chaotic patterns, the velocity $v(t)$ and phase, (t) of pulled fronts which emerge from steep initial conditions (falling off faster than $e^{-\lambda^* x}$ for $x \to \infty$), display a *universal* power law relaxation with time t, expressed by

$$v(t) \equiv v^* + \dot{X}(t) \tag{1}$$

$$\dot{X}(t) = -\frac{3}{2\lambda^* t} + \frac{3\sqrt{\pi}}{2\lambda^{*2} t^{3/2}}\mathrm{Re}\left(\frac{1}{\sqrt{D}}\right) + \mathcal{O}\left(\frac{1}{t^2}\right) , \tag{2}$$

$$, (t) = -q^* \dot{X}(t) - \frac{3\sqrt{\pi}}{2\lambda^* t^{3/2}}\mathrm{Im}\left(\frac{1}{\sqrt{D}}\right) + \mathcal{O}\left(\frac{1}{t^2}\right) . \tag{3}$$

As explained below, the coefficients $v^*, k^* = q^* + i\lambda^*$, and D are all given explicitly in terms of the dispersion relation of the linearized equation. We shall focus on determining how these exact asymptotic relaxation formulas emerge, and why they are independent of the nonlinearities, the precise initial conditions, or on whether the front dynamics is regular or chaotic. Before embarking on this, however, it is important to explain what we mean by velocity and phase for the various types of fronts.

Uniformly translating pulled fronts. The simplest types of fronts are those for which the dynamical field $\phi(x,t)$ asymptotically approaches a uniformly translating profile $\phi \equiv \Phi_{v^*}(\xi)$, $\xi = x - v^* t$, as happens, e.g., in the celebrated nonlinear diffusion equation $\partial_t \phi = \partial_x^2 \phi + \phi - \phi^3$ for

fronts propagating into the unstable $\phi = 0$ state. If we define *level curves* as the lines in an x, t diagram where $\phi(x,t)$ has a particular value, we can define the velocity $v(t)$ as the slope of a level curve. For *uniformly translating fronts*, $q^* = 0 = \mathrm{Im}D$; (2) then reduces to the expression derived for uniformly translating fronts in [7]. The remarkable point is that the expression for $v(t)$ is in this case completely independent of which level curve one traces. Moreover, it was shown in [7] that the nonlinear front region is slaved to the leading edge of the front whose velocity relaxes according to (2). This results in

$$\phi(x,t) = \Phi_{v(t)}(\xi_X) + \mathcal{O}(t^{-2}) , \quad \xi_X \ll \sqrt{t} , \tag{4}$$

$$\xi_X = x - v^* t - X(t) , \tag{5}$$

where $\Phi_v(\xi)$, $\xi = x - vt$ solves the *o.d.e.* for a front propagating uniformly with velocity v. $v(t)$ in (4) is the instantaneous velocity of the front, and the frame ξ_X is shifted by the time dependent quantity $X(t)$. Since the collective coordinate $X(t)$ diverges as $\ln t$ for large t according to (2), the difference between ξ_X and a uniformly translating frame is crucial — only in the former can we follow the relaxation. Uniformly translating fronts have no phase, hence all terms in (3) vanish identically.

Coherent pattern generating fronts. As an example of coherent pattern generating fronts, we consider the so-called Swift-Hohenberg (SH) equation

$$\partial_t u = \varepsilon u - (1 + \partial_x^2)^2 u - u^3 , \quad \varepsilon > 0 . \tag{6}$$

The space-time plot of Fig. 1(a) illustrates how SH-fronts with steep initial conditions (falling off faster than $e^{-\lambda^* x}$ as $x \to \infty$ into the unstable state $u = 0$) generate a periodic pattern. It is known that they are pulled [4,8,9]. In this case, new level curves in an x, t plot are constantly being generated. If we define in this case the velocity as the slope of the uppermost level curve, one gets an oscillatory function. Its average is $v(t)$ given in (1), but $v(t)$ is difficult to extract this way. Numerically, it is better to determine the velocity from an empirical envelope obtained by interpolating the positions of the maxima. Since these pattern forming front solutions for long times have a temporal periodicity $u(\xi, t) = u(\xi, t + T)$ in the frame $\xi = x - vt$ moving with the velocity v of the front, the asymptotic profiles can be written in the form $\sum_{n=1} e^{-2\pi i n t/T} U_v^n(\xi) + c.c.$. In terms of these complex modes U, our result for the shape relaxation of the pulled front profile becomes in analogy to (4)

$$u(x,t) \simeq \sum_{n=1} e^{-ni\Omega^* t - ni\Gamma(t)} U_{v(t)}^n(\xi_X) + c.c. + \cdots \tag{7}$$

with the frequency Ω^* given below [10]. Eq. (7) shows that , (t) is the *global phase* of the relaxing profile, as the functions U_v^n only have a ξ_X-dependence. The result of our calculation of the long time relaxation of $v(t)$ and , (t) is given in (1) − (3). We stress that while for $\varepsilon \to 0$,

an ansatz like (7) leads to an amplitude equation for the $n = \pm 1$ terms, our analysis applies for *any* $\varepsilon > 0$.

Incoherent or chaotic fronts. The third class we consider consists of fronts which leave behind chaotic states. They occur in some regions of parameter space in the cubic Complex Ginzburg-Landau equation [11] or in the quintic extension (QCGL) [12] that we consider here,

$$\partial_t A = \varepsilon A + (1 + iC_1)\partial_x^2 A + (1 + iC_3)|A|^2 A \\ - (1 - iC_5)|A|^4 A \ . \qquad (8)$$

Fig. 1*(b)* shows an example of a pulled front in this equation. Level curves in a space-time diagram can now also both start and end. If we calculate the velocity from the slope of the uppermost level line, then its average value is again given by (2) [13], but the oscillations can be quite large. However, our analysis confirms what is already visible in Fig. 1*(b)*, namely that even a chaotic pulled front becomes more coherent the further one looks into the leading edge of the profile. Indeed we will see that in the leading edge where $|A| \ll 1$ the profile is given by an expression reminiscent of (7),

$$A(x,t) \approx e^{-i\Omega^* t - i\Gamma(t)} e^{ik^* \xi_X} \psi(\xi_X), \quad 1 \ll \xi_X \ll \sqrt{t}. \quad (9)$$

The fluctuations about this expression become smaller the larger ξ_X.

In Figs. 1*(c)* and 2*(c)* we show as an example results of our simulations of the SH equation (6) and the QCGL (8). They fully confirm our predictions (2) and (3) for the asymptotic average velocity and phase relaxation. Note that for the QCGL, the fluctuations are indeed smaller the more one probes the leading edge region.

We now summarize how these results arise.

Calculation of the asymptotic parameters. Although this is well-known [14], we first briefly summarize how the linear spreading velocity v^* and the associated parameters λ^* etc. arise, as the analysis also motivates the subsequent steps. After linearization about the unstable state, the equations we consider can all be written in the form $\partial_t \phi = \mathcal{L}(\partial_x, \partial_x^2, \cdots)\phi$. For a Fourier mode $e^{-i\omega t + ikx}$, this yields the dispersion relation $\omega(k)$. The linear spreading velocity v^* of steep initial conditions is then obtained by a saddle point analysis of the Green's function G of these equations. In the asymptotic frame $\xi = x - v^* t$, $G(\xi, t)$ becomes

$$G(\xi,t) = \int \frac{\mathrm{d}k}{2\pi} e^{-i\Omega(k)t + ik\xi} \approx e^{ik^* \xi - i\Omega^* t} \frac{e^{-\frac{\xi^2}{4Dt}}}{\sqrt{4\pi Dt}} \quad (10)$$

for large times. Here $\Omega(k) = \omega(k) - v^* k$, and

$$\left.\frac{\mathrm{d}\Omega(k)}{\mathrm{d}k}\right|_{k^*} = 0 \ , \quad \mathrm{Im}\,\Omega(k^*) = 0 \ , \quad D = \left.\frac{i\mathrm{d}^2\Omega(k)}{2\mathrm{d}k^2}\right|_{k^*} \ . \quad (11)$$

The first equation in (11) is the saddle point condition, while the second one expresses the self-consistency condition that there is no growth in the co-moving frame.

These equations straight forwardly determine $v^*, k^* = q^* + i\lambda^*, D$ and the real frequency $\Omega^* = \Omega(k^*)$ [15].

Choosing the proper frame and transformation. Eq. (10) not only confirms that a localized initial condition will grow out and spread asymptotically with the velocity v^* given by (11), but the Gaussian factor also determines how the asymptotic velocity is approached in the fully linear case. Our aim now is to understand the convergence of a pulled front due to the interplay of the linear spreading and the nonlinearities. The Green's function expression (10) gives three important hints in this regard: First of all, $G(\xi,t)$ is asymptotically of the form $e^{ik^* \xi - i\Omega^* t}$ *times* a crossover function whose diffusive behavior is betrayed by the Gaussian form in (10). Hence if we write our dynamical fields as $A = e^{ik^* \xi - i\Omega^* t}\psi(\xi, t)$ for the QCGL (8) or $u = e^{ik^* \xi - i\Omega^* t}\psi(\xi, t) + c.c.$ for the real field u in (6), we expect that the dynamical equation for $\psi(\xi, t)$ obeys a diffusion-type equation. Second, as we have argued in [7], for the relaxation analysis one wants to work in a frame where the crossover function ψ becomes asymptotically time independent. This is obviously not true in the ξ frame, due to the factor $1/\sqrt{t}$ in (10). However, this term can be absorbed in the exponential prefactor, by writing $t^{-\nu} e^{ik^* \xi - i\Omega^* t} = e^{ik^* \xi - i\Omega^* t - \nu \ln t}$. Hence, we introduce the logarithmically shifted frame $\xi_X = \xi - X(t)$ [7] as already used in (5). Third, we find a new feature specific for pattern forming fronts: the complex parameters, and D in particular, lead us to introduce the global phase $\dot{\Gamma}(t)$. We expand $\dot{\Gamma}(t)$ like $\dot{X}(t)$ [7]

$$\dot{X}(t) = \frac{c_1}{t} + \frac{c_{3/2}}{t^{3/2}} + \cdots , \quad \dot{\Gamma}(t) = \frac{d_1}{t} + \frac{d_{3/2}}{t^{3/2}} + \cdots \quad (12)$$

and analyze the long time dynamics by performing a "leading edge transformation" to the field ψ,

$$\begin{aligned} \text{QCGL:} \quad & A = e^{ik^* \xi_X - i\Omega^* t - i\Gamma(t)}\,\psi(\xi_X, t) \ , \\ \text{SH:} \quad & u = e^{ik^* \xi_X - i\Omega^* t - i\Gamma(t)}\,\psi(\xi_X, t) + c.c. \quad (13) \end{aligned}$$

Steep initial conditions imply that $\psi(\xi_X, t) \to 0$ as $\xi_X \to \infty$. The determination of the coefficients in the expansions (12) of $\dot{X}$ and $\dot{\Gamma}$ is the main goal of the subsequent analysis, as this then directly yields Eqs. (2) and (3).

Understanding the intermediate asymptotics. Substituting the leading edge transformation (13) into the nonlinear dynamical equations, we get

$$\partial_t \psi = D\partial_{\xi_X}^2 \psi + \sum_{n=3} D_n \partial_{\xi_X}^n \psi \\ + [\dot{X}(t)(\partial_{\xi_X} + ik^*) + i\dot{\Gamma}(t)]\psi - N(\psi) \ , \qquad (14)$$

with $D_n = (-i/n!)\mathrm{d}^n\Omega/(\mathrm{d}ik)^n|_{k^*}$ the generalization of D in (11) (of course, for the QCGL, $\Omega(k)$ is quadratic in k, so $D_n = 0$). In this equation, N accounts for the nonlinear terms; e.g., for the QCGL, we simply have

3

$$N = e^{-2\lambda^*\xi_X}|\psi|^2\psi \left[1 - iC_3 + (1 - iC_5)e^{-2\lambda^*\xi_X}|\psi|^2\right] . \quad (15)$$

The expression for the SH equation is similar.

The structure of Eq. (14) is that of a diffusion-type equation with $1/t$ and higher order corrections from the $\dot{X}$ and $\dot{,}$ terms, and with a nonlinearity N. The crucial point to recognize now is that for fronts, N is nonzero *only in a region of finite width*: For $\xi_X \to \infty$, N decays exponentially due to the explicit exponential factors in (15). For $\xi_X \to -\infty$, N also decays exponentially, since u and A remain finite, so that ψ decays as $e^{-\lambda^*|\xi_X|}$ according to (13). Intuitively, therefore, we can think of (14) as a diffusion equation in the presence of a sink N localized at some finite value of ξ_X. The ensuing dynamics of ψ to the right of the sink can be understood with the aid of Figs. 2 *(a)* and *(b)*, which are obtained directly from the time-dependent numerical simulations of the QCGL (8). To extract the intermediate asymptotic behavior illustrated by these plots, we integrate (14) once to get

$$\partial_t \int_{-\infty}^{\xi_X} \mathrm{d}\xi'_X\, \psi = D\partial_{\xi_X}\psi + \sum_{n=3} \frac{D_n}{n-1}\, \partial_{\xi_X}^{n-1}\psi + \quad (16)$$

$$+ i[k^*\dot{X}(t) + \dot{,}(t)] \int_{-\infty}^{\xi_X} \mathrm{d}\xi'_X\, \psi + \dot{X}(t)\psi - \int_{-\infty}^{\xi_X} \mathrm{d}\xi'_X\, N(\psi)$$

Now, in the region labeled I in Fig. 2 *(b)*, we have for fixed ξ_X and $t \to \infty$ that the terms proportional to $\dot{X}$ and $\dot{,}$ can be neglected upon averaging over the fast fluctuations; the same holds for the term on the left. Since the integral converges quickly to the right due to the exponential factors in N, we then get immediately, irrespective of the presence of higher order spatial derivatives

$$\lim_{t\to\infty} D\,\overline{\frac{\partial\psi}{\partial\xi_X}} = \int_{-\infty}^{\infty} d\xi_X\, \overline{N(\psi)} \equiv \alpha D . \quad (17)$$

Here, the overbar denotes a time average (necessary for the case of a chaotic front). Thus, for large times in region I, $\overline{\psi} \approx \alpha\xi_X + \beta$ in dominant order. Moreover, from the diffusive nature of the equation, our assertion that the fluctuations of ψ rapidly decrease to the right of the region where N is nonzero comes out naturally. In other words, provided that the time-averaged sink strength α is nonzero, $\alpha \neq 0$, one will find a buildup of a linear gradient in $|\overline{\psi}|$ in region I, *independent of the precise form of the nonlinearities or of whether or not the front dynamics is coherent*. This behavior is clearly visible in Fig. 2 *(b)*. We can understand the dynamics in regions II and III along similar lines. In region III the dominant terms in (14) are the one on the left and the first one on the second line, and the cross-over region II which separates regions I and III moves to the right according to the diffusive law $\xi_X \sim D\sqrt{t}$.

Systematic expansion. These considerations are fully corroborated by our extension of the analysis of [7]. Anticipating that ψ falls off for $\xi_X \gg 1$, we split off a Gaussian factor by writing $\psi(\xi_X, t) = G(z, t)\, e^{-z}$ in terms of the similarity variable $z = \xi_X^{*2}/(4Dt)$, and expand

$$G(z, t) = t^{1/2}g_{-\frac{1}{2}}(z) + g_0(z) + t^{-1/2}g_{\frac{1}{2}}(z) + \cdots \quad (18)$$

This, together with the expansion (12) for $X(t)$ and $,(t)$, the left "boundary condition" that $\psi(\xi_X, t\to\infty) = \alpha\xi_X + \beta$ and the condition that the functions $g(z)$ do not diverge exponentially, then results in the expressions (2) for $\dot{X}(t)$ and (3) for $\dot{,}$ [9]. For the QCGL, the analysis immediately implies the result (9) for the front profile in the leading edge. In addition for the SH equation, one arrives at (7) for the shape relaxation in the front interior along the lines of [7]: Starting from the *o.d.e.*'s for the U_v^n, one finds upon transforming to the frame ξ_X that to $\mathcal{O}(t^{-2})$, the time dependence only enters parametrically through $v(t)$. This then yields (7).

In conclusion, we have shown that the long time relaxation of pulled fronts is remarkably universal: Independent of whether fronts are uniformly translating, pattern generating or chaotic, the velocity and phase relaxation is governed by one simple formula, with universal dominant and subdominant power law expressions.
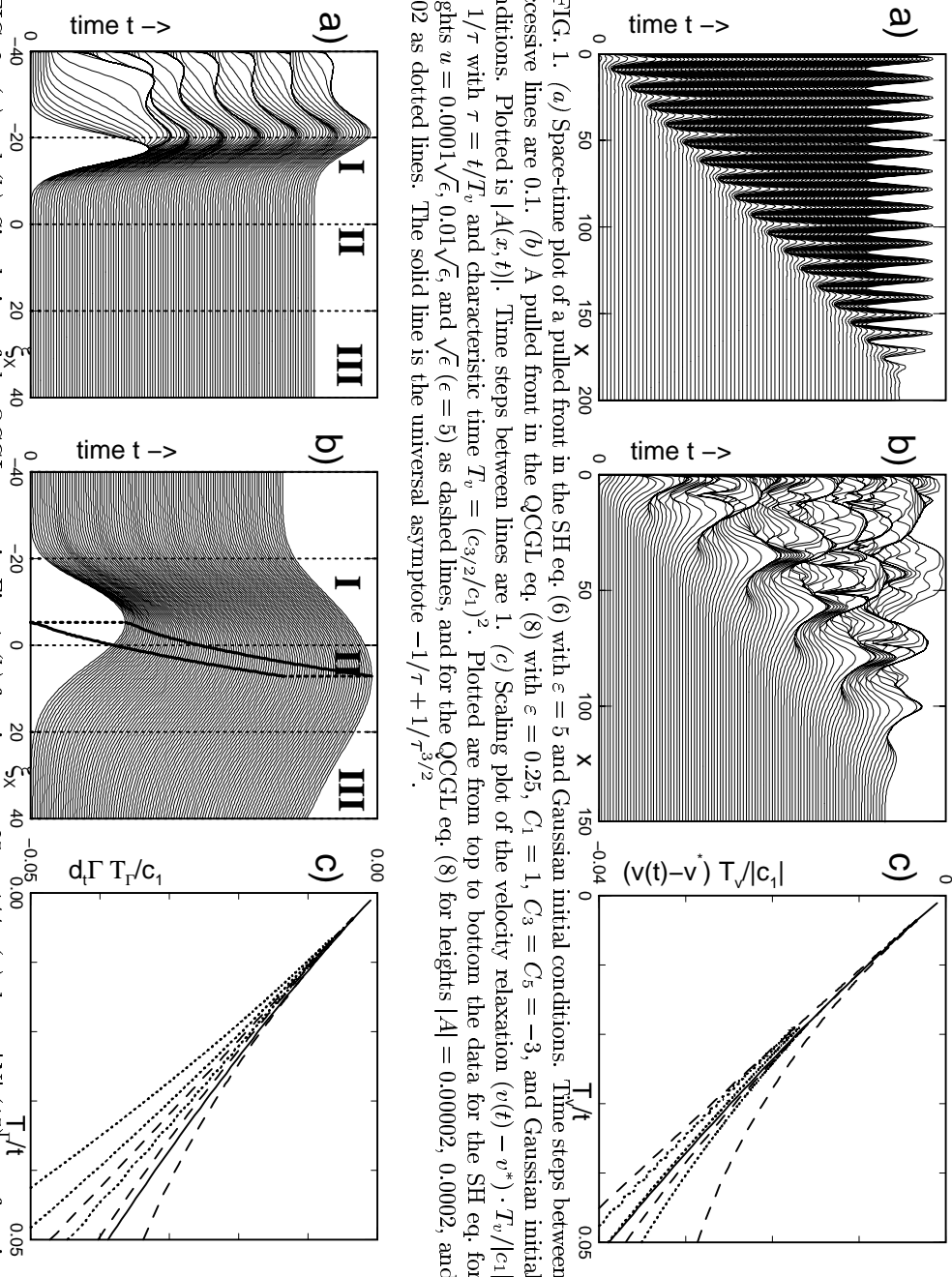
FIG. 1. (a) Space-time plot of a pulled front in the SH eq. (6) with $\epsilon = 5$ and Gaussian initial conditions. Time steps between successive lines are 0.1. (b) A pulled front in the QCGL eq. (8) with $\epsilon = 0.25$, $C_1 = 1$, $C_3 = C_5 = -3$, and Gaussian initial conditions. Plotted is $|A(x,t)|$. Time steps between lines are 1. (c) Scaling plot of the velocity relaxation $(v(t) - v^*) \cdot T_v/|c_1|$ vs. $1/\tau$ with $\tau = t/T_v$ and characteristic time $T_v = (c_{3/2}/c_1)^2$. Plotted are from top to bottom the data for the SH eq. for heights $u = 0.0001\sqrt{\epsilon}$, $0.01\sqrt{\epsilon}$, and $\sqrt{\epsilon}$ ($\epsilon = 5$) as dashed lines, and for the QCGL eq. (8) for heights $|A| = 0.00002$, 0.0002, and 0.002 as dotted lines. The solid line is the universal asymptote $-1/\tau + 1/\tau^{3/2}$.
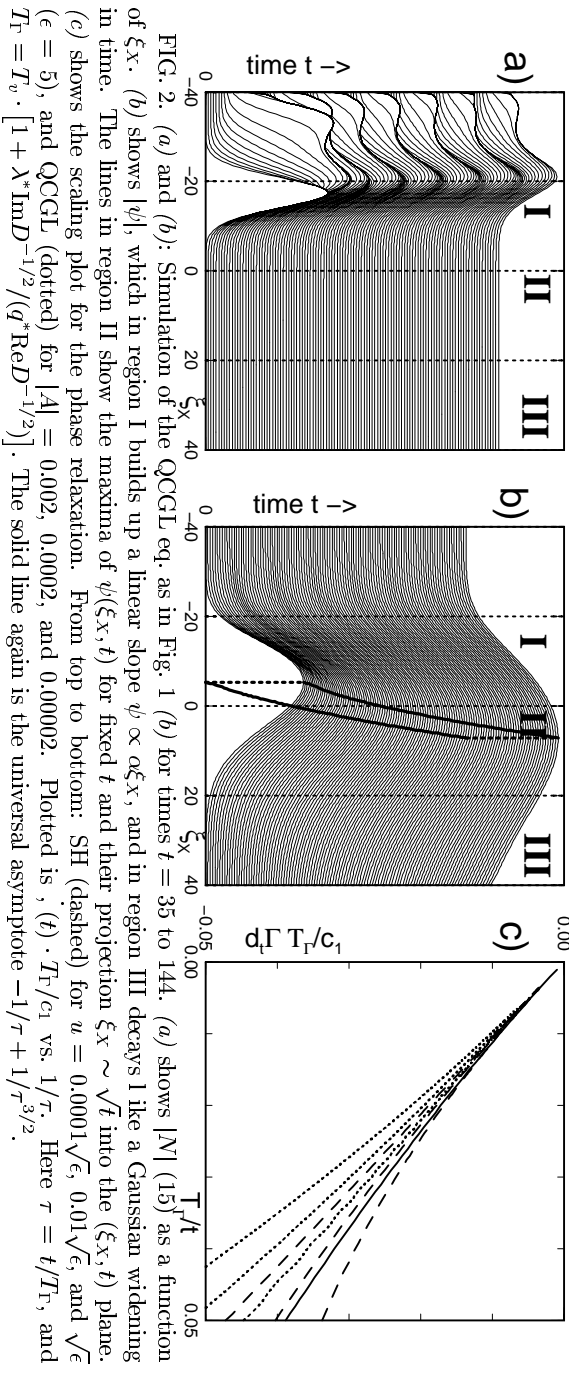

FIG. 2. (a) and (b): Simulation of the QCGL eq. as in Fig. 1 (b) for times $t = 35$ to 144. (a) shows $|N|$ (15) as a function of ξ_x. (b) shows $|\psi|$, which in region I builds up a linear slope $\psi \propto \alpha\xi_x$, and in region III decays l like a Gaussian widening in time. The lines in region II show the maxima of $\psi(\xi_x, t)$ for fixed t and their projection $\xi_x \sim \sqrt{t}$ into the (ξ_x, t) plane. (c) shows the scaling plot for the phase relaxation. From top to bottom: SH (dashed) $d_t\Gamma \cdot T_\Gamma/c_1$ vs. $1/\tau$, and QCGL (dotted) for $|A| = 0.002$, 0.0002, and 0.00002. Plotted is , $(t) \cdot T_\Gamma/c_1$ vs. $1/\tau$. Here $\tau = t/T_\Gamma$, and $T_\Gamma = T_v \cdot [1 + \lambda^* \mathrm{Im} D^{-1/2}/(q^* \mathrm{Re} D^{-1/2})]$. The solid line again is the universal asymptote $-1/\tau + 1/\tau^{3/2}$.

5

[1] M. C. Cross and P. C. Hohenberg, Rev. Mod. Phys. **65**, 851 (1993).

[2] J.D. Murray, *Mathematical Biology* (Springer, Berlin, 1989).

[3] E. Ben-Jacob, H.R. Brand, G. Dee, L. Kramer, and J.S. Langer, Physica D **14**, 348 (1985).

[4] W. van Saarloos, Phys. Rev. A **39**, 6367 (1989).

[5] A. N. Stokes, Math. Biosci. **31**, 307 (1981).

[6] G. C. Paquette, L.-Y. Chen, N. Goldenfeld and Y. Oono, Phys. Rev. Lett. **72**, 76 (1994).

[7] U. Ebert and W. van Saarloos, Phys. Rev. Lett. **80**, 1650 (1998); preprint submitted to Physica D.

[8] G. Dee and J. S. Langer, Phys. Rev. Lett. **50**, 383 (1983).

[9] U. Ebert, W. Spruijt and W. van Saarloos (unpublished).

[10] Underlying (7) is the assumption that the (6) admits a two-parameter family of front solutions. This was shown for small ϵ by P. Collet and J.-P. Eckmann, Commun. Math. Phys. **107**, 39 (1986), and is demonstrated by counting arguments for arbitrary ϵ in [9].

[11] K. Nozaki and N. Bekki, Phys. Rev. Lett. **51**, 271 (1983).

[12] W. van Saarloos and P. C. Hohenberg, Physica D **56**, 303 (1992).

[13] This is true for chaotic fronts provided that the temporal correlation function for the chaotic variable falls off at least as fast as t^{-2}, so that the temporal change of the average velocity $v(t)$ can be considered adiabatically.

[14] E. M. Lifshitz and L.P. Pitaevskii, *Physical Kinetics* (Pergamon, New York, 1981).

[15] For (8), $v^* = 2\sqrt{\epsilon/(1 + C_1^2)}$ and $D = (C_1 + i)/(1 + iC_1)$. For (6), $\lambda^* = [(\sqrt{1 + 6\epsilon} - 1)/12]^{1/2}$, $q^* = \pm\sqrt{\sqrt{1 + 3\lambda^{*2}}}$, $v^* = 8\lambda^*(1 + 4\lambda^{*2})$, $\Omega^* = -C_1\epsilon$ and $k^* = (C_1 + i)\sqrt{\epsilon/(1 + C_1^2)}$, $\Omega^* = -8\lambda^* q^{*3}$, $D = 4q^{*2} + 12iq^*\lambda^*$.